Phonon-libron dynamics of acetylene adsorbed on NaCl(001)

S. Picaud, P. N. M. Hoang, and C. Girardet*
Laboratoire de Physique Moléculaire UMR CNRS 6624, Faculté des Sciences, La Bouloie, Université de Franche-Comté, 25030 Besançon Cedex, France

A. Glebov, R. E. Miller,† and J. P. Toennies
Max-Planck-Institut für Strömungsforschung, Bunsenstrasse 10, D-37073 Göttingen, Germany
(Received 1 December 1997)

The phonon-dispersion curves of the high-temperature $(3\sqrt{2}\times\sqrt{2})R45°$ phase of acetylene on NaCl(001) have been measured using high-resolution time-of-flight inelastic helium-atom scattering and compared with semiempirical calculations. The observed two Einstein vibrational modes at 8 and 14 meV are assigned to a collective perpendicular motion of the molecule centers of mass in the monolayer and to a collective librational motion of the molecular axes, respectively. With the same semiempirical potential used in the dynamical calculations, the 0 K adsorbate monolayer structure is predicted to be $(\sqrt{2}\times\sqrt{2})R45°$ which is at variance with the $(7\sqrt{2}\times\sqrt{2})R45°$ structure determined at $T<80$ K by helium diffraction. The results are compared with structure assignments based on infrared spectroscopy and *ab initio* calculations. [S0163-1829(98)04216-7]

I. INTRODUCTION

In recent years, the physisorption of polar molecules such as CO, OCS, NH_3, and H_2O on NaCl or MgO single-crystal substrates has been widely studied both theoretically[1–15] and experimentally.[16–23] These results reveal that the bonding is governed by rather complex force fields that depend strongly on both the electrostatic properties of the admolecules as well as on the electric fields and field gradients produced by the ions of the substrate.[24] *Ab initio* potential energy calculations have provided additional insight into the adsorption characteristics of such systems.[7,8,11,12] Unfortunately, they are often very time consuming and their reliability becomes questionable when the systems are large. Minimization procedures applied to semiempirical potentials are often more suitable for studying systems with a large number of degrees of freedom. Some recent studies on the CO/MgO (Refs. 9 and 10) and OCS/NaCl (Ref. 23) systems have nicely illustrated the complementarity of experiments and theoretical calculations for obtaining a complete understanding of the structure and dynamics of physisorbed molecular monolayers.

In the present work, helium-atom scattering (HAS) in combination with dynamical calculations is employed to investigate the structure and the libron-phonon modes of acetylene molecules on NaCl(001). The HAS technique has the advantage of being insensitive to surface charging and provides both structural information via diffraction patterns and information on the surface phonon mode dispersion curves. The C_2H_2/NaCl system has been extensively studied in recent years by *ab initio* approaches,[8] HAS (Ref. 22), and polarization infrared spectroscopy (PIRS) (Ref. 19), which gives information on the internal vibrations of the admolecules and on their orientations with respect to the surface.[16,19,20] PIR spectroscopy of C_2D_2 and C_2H_2 layers adsorbed on NaCl(100) revealed that the *p* and *s* polarized spectra of the asymmetric stretching vibrations (ν_3) are quite similar at 78 K, exhibiting a high-frequency singlet and a low-frequency doublet.[19] A bilayer model with two sublattices, one associated with a full monolayer producing the doublet and the second corresponding to a half-filled second layer giving rise to the singlet, was proposed to explain the PIRS data. In both sublattices, the molecular axes were proposed to be nearly planar above the surface, with a tilt angle of around 80°. In the first layer, the neighboring molecules were assumed to be arranged in a *T*-shaped pattern.[19]

Periodic Hartree-Fock calculations have been reported at two surface coverages, namely, 0.25 ML and 1.0 ML.[8] At low coverage, the C_2H_2 molecules were found to lie flat on the surface, with their centers of mass above the Na^+ cations and their symmetry axes directed either along Na rows or along Na-Cl-Na rows. At a monolayer coverage a $(\sqrt{2}\times\sqrt{2})R45°$ unit cell was predicted at $T_s=0$ K with two mutually perpendicular molecules lying above adjacent cations.

The helium-atom diffraction results on the structural properties of acetylene on NaCl, presented in a previous paper,[22] clearly showed the existence of two monolayer phases, depending upon the coverage and temperature. At $T_S=90$ K, a stable low-density phase (phase I) was observed, characterized by a rotated $(3\sqrt{2}\times\sqrt{2})R45°$ unit cell, presumably containing four molecules. At $T_S=80$ K, the growth continued beyond phase I leading to a higher-density phase II, with a $(7\sqrt{2}\times\sqrt{2})R45°$ unit mesh, corresponding to the full monolayer. At 50 K, phase II was formed directly and phase I was not observed. Since none of the unit cells are consistent with the bilayer model constructed on the basis of the PIRS measurements,[19] new structures were proposed[22] that could quite nicely explain all of the available data.

This article is organized in the following way. The experimental time-of-flight scattering spectra and their analysis are presented in Sec. II. Section III describes the theory used in the study of both the structure and the dynamics of the acetylene layer. In Sec. IV, the results are discussed and compared to previous assignments based on the infrared experiments of Dunn and Ewing[19] and the previous *ab initio* calculations.[8]

II. INELASTIC HELIUM ATOM SCATTERING RESULTS

The HAS apparatus used in the present work was described in detail elsewhere.[26] A nearly monoenergetic He beam ($\Delta E/E \leqslant 2\%$) is produced by a continuous expansion of helium gas through the 10-μm nozzle. The beam passes through a skimmer followed by a chopper for time-of-flight (TOF) measurements and then collides with the crystal surface in the target chamber. After a time-of-flight path of 143 cm the scattered He atoms are detected by a magnetic mass spectrometer operated in a single ion counting mode. The base pressure was less than 5×10^{-11} mbar in both the target and detector chambers.

The NaCl crystal target (Karl Korth Kristalle GmbH, Am Jägersberg 3, D-24161 Altenholz, Germany) used in this work had dimensions of $10\times10\times10$ mm^3 prior to the cleavage and was cleaved in vacuum at a crystal temperature of $T_s=100$ K. The crystal temperature was measured with a NiCr/Ni thermocouple located in a small hole drilled into the side of the crystal about 1 mm from the surface. The acetylene purification procedure is described in Ref. 22, where the details on the growth, formation and unit mesh symmetries of the two acetylene phases are also given.

From each TOF spectrum, the energies ($\hbar\omega$) of the phonons can be easily identified and the associated parallel wave vector transfer ($\Delta\mathbf{K}$) can be calculated from the conservation equations. This analysis can be facilitated by referring to a scan curve that relates all possible wave-vector transfers ($\Delta\mathbf{K}$) and energy transfers ($\hbar\omega$) with the incident angle (Θ_i) and the initial parallel wave vector component $\mathbf{K}_i=\mathrm{k}_i \sin\Theta_i$, as

$$\hbar\omega=-E_i+E_i\left(1+\frac{\Delta\mathbf{K}}{\mathbf{K}_i}\right)^2\frac{\sin^2\Theta_i}{\sin^2\Theta_f}. \tag{1}$$

In this apparatus the angle between the incident beam and the scattered is fixed at $\Theta_{SD}=90.1°$ and thus the sum of the incident (Θ_i) and final (Θ_f) angles, measured with respect to the surface normal, is given by $\Theta_i+\Theta_f=90.1°$.

The present experiments were carried out on the high-temperature $(3\sqrt{2}\times\sqrt{2})R45°$ phase I of acetylene on NaCl(001) along two symmetry directions, namely, $\langle100\rangle$ and $\langle110\rangle$. The detailed diagrams representing the reciprocal and direct space lattices of this phase can be found in Ref. 22. The adlayer was formed at 90 K and then it was cooled to 70 K after removing the gas phase overpressure. Owing to the low Debye temperatures associated with these physisorbed layers,[27] the lowest possible temperature was used in order to reduce the background from multiphonon scattering. The inelastic scattering measurements were carried out by recording TOF spectra at about 100 incident angles in two directions. Each spectrum required approximately 30–40 min of signal averaging. The layers were desorbed every 8–10 h and regrown in order to avoid a buildup of contaminants. A number of representative TOF spectra measured at an incident helium beam energy of 20.1 meV for different incident angles every 0.5° between the first-order diffraction peaks along the $\langle100\rangle$ direction are shown in Fig. 1. For clarity, the spectra have already been transformed to an energy transfer scale.

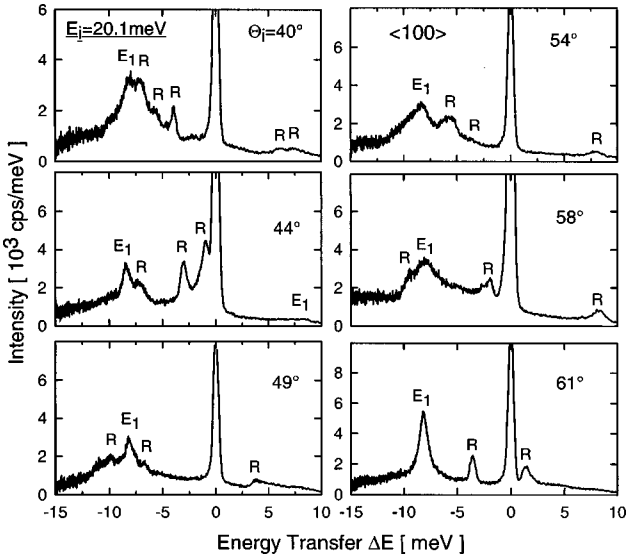

FIG. 1. A series of representative TOF spectra converted to the energy transfer scale for phase I in the $\langle100\rangle$ direction. The measurements were carried out at $T_S=70$ K and $E_i=20$ meV. The Rayleigh mode of the substrate is labeled by R. The Einstein-like mode E_1 is assigned to frustrated translations of the acetylene molecules.

As evident from Fig. 1, the most pronounced phonon peaks in the TOF spectra are those at negative energies that correspond to creation events as expected at low crystal temperatures.[28] The rather intense diffuse elastic peak observed at zero energy transfer, which is due to incoherent scattering from surface defects,[29] indicates a rather significant density of defects in the adlayer.

Figure 2 shows the surface phonon-dispersion curves for the adsorbed layer in an extended zone diagram of the substrate surface that were constructed using the scan curve [Eq. (1)]. The measured points are indicated by the open circles and the vertical dotted-dashed lines indicate the positions of

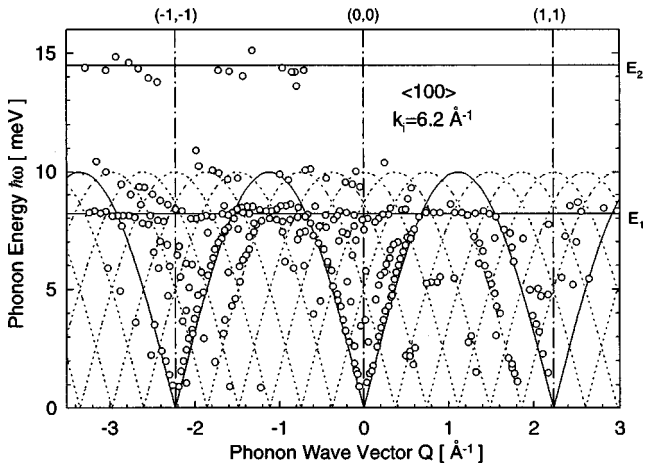

FIG. 2. Surface phonon dispersion curves for phase I of acetylene in the $\langle100\rangle$ direction. The open circles are the measured points. The dotted-dashed lines correspond to the centers of the substrate Brillouin zones ($\bar{\Gamma}$ points). The solid sine curves are models of the clean NaCl substrate Rayleigh modes, while the dotted sine curves are for the same substrate Rayleigh modes, folded with the **G** vectors of the adlayer superstructure (*Umklapp* processes).

the Bragg diffraction peaks from the NaCl(100) surface, corresponding to the centers of the unreconstructed surface Brillouin zones ($\bar{\Gamma}$ points). In this direction the dispersion curves are repeated six times for each reciprocal lattice vector of the clean unreconstructed NaCl(100) surface due to the large unit mesh of the phase I acetylene overlayer. The dispersion of the Rayleigh modes of NaCl(100) is well known and was measured using helium-atom scattering in earlier experiments.[30] As a simple model, these modes are presented in Fig. 2 as sine curves, with an amplitude of 10 meV corresponding to the energy at the Brillouin-zone boundary ($\bar{M}$ point). The solid curve corresponds to the Rayleigh mode associated with the integer order diffraction peaks, while the dotted sine curves represent those of fractional order (specifically the sixth order). Indeed, the Rayleigh modes appear as folded due to *Umklapp* processes via a reciprocal lattice vector of the superstructure unit cell of the overlayer. In the present case $|\mathbf{G}_{\text{adsorbate}}| = \frac{1}{6}|\mathbf{G}_{\text{NaCl}}|$. The specular and first order Rayleigh modes are clearly seen along the entire phonon wave vector $\mathbf{Q}$ region. In contrast, the fractional order modes are only visible in certain regions, for example, where the modes are next to the first-order diffraction peaks at $\mathbf{Q} = \pm 1.93\ \text{Å}^{-1}$.

Although, to our knowledge, this is the first measurement of folded Rayleigh modes on an insulator surface, this effect has already been observed by helium scattering for several systems such as Cu/Si(111) (Ref. 31) and Si(111)-(7×7) (Ref. 32) surfaces. In both cases, the intensities of the Rayleigh modes were observed to be proportional to the elastic intensities of the associated Bragg diffraction peaks, as observed in the present case.

In addition, the horizontal solid line in Fig. 2 labeled E_1 indicates a nearly dispersionless mode at an energy of approximately 8.2 meV. A relatively small number of points along the line labeled E_2 indicate the existence of a second phonon mode (most likely Einstein-like) at 14.5 meV. Unfortunately, these peaks were very weak in the spectrum and the data are not sufficiently complete to make a definitive statement about the dispersion of this mode.

Similar TOF measurements were performed on phase I of C_2H_2/NaCl(001) in the other high-symmetry direction ⟨110⟩. Ten (out of a total of 40) TOF spectra are depicted in Fig. 3. As in the case of the ⟨100⟩ direction (Fig. 1) a rather large diffuse elastic peak is observed, indicating the presence of surface defects in the adsorbate layer. Once again, the phonons are predominantly on the phonon creation sides of the spectra ($\Delta E < 0$). A fairly broad phonon peak is clearly visible in all of the spectra at the energy of $\hbar\omega = 8.2$ meV. Some sharper peaks that change their position with the incident angle Θ_i are assigned to the substrate Rayleigh wave. The phonon dispersion curves derived from the TOF spectra for the C_2H_2 monolayer along the ⟨110⟩ direction, are plotted in Fig. 4.

It should be noted that in this direction no superstructure peaks were observed and, hence, no *Umklapp* processes with the adsorbate reciprocal unit vectors are expected. Thus, the phonon-dispersion curves presented in Fig. 4 were folded into the Brillouin zone of the NaCl substrate. A sine model of the NaCl Rayleigh mode is shown by the dashed line and is labeled RW_{NaCl}. It is apparent from the figure that the RW

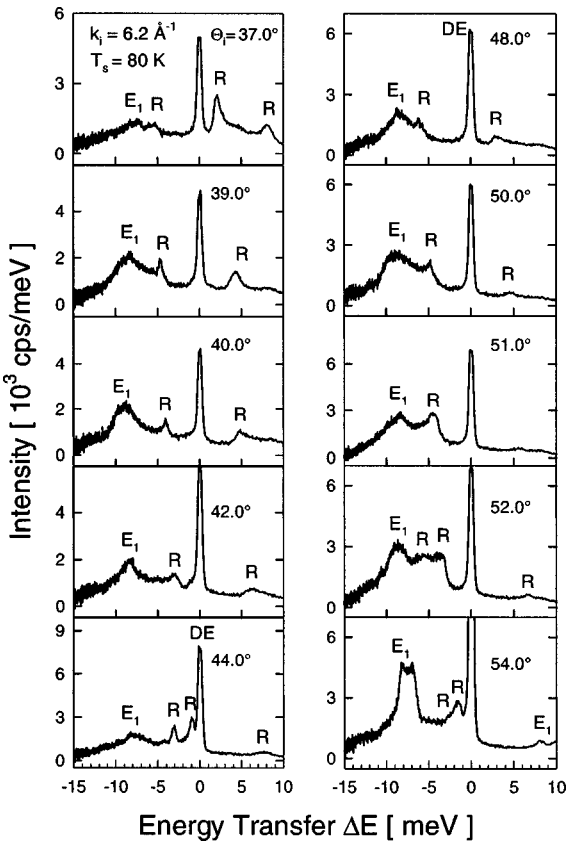

FIG. 3. A series of representative TOF spectra, converted to the energy transfer scale, for phase I in the ⟨110⟩ direction measured at ten different incident angles Θ_i. The measurements were carried out at $T_s = 80$ K and $E_i = 20$ meV. The diffuse elastic peak at zero energy transfer is labeled DE. Several phonon peaks are observed in each spectrum predominantly on the phonon creation side.

is observed along the entire Brillouin zone with significantly lower intensity above the E_1 mode. As in the ⟨100⟩ direction, two Einstein modes E_1 and E_2 are visible. Mode E_1 is very intense and rather broad, while the second Einstein mode is weak. Due to the low signals, it was not possible to determine whether or not the E_2 mode displayed dispersion. The energies of both Einstein modes are the same as in the ⟨100⟩ direction, namely, $\hbar\omega_{E_1} = 8.2$ meV and $\hbar\omega_{E_2} \approx 14.5$ meV.

The Einstein oscillator mode E_1 could be due to a frustrated translation or rotation of the acetylene molecules on the surface. Similar dispersionless adsorbate phonon modes have been observed previously for a number of other monolayer systems.[6,25] In spite of the lack of sufficient signal to determine any dispersion of the E_2 mode, it is also tentatively assigned to some form of frustrated adsorbate vibrational motions. Additional information on the identities of these modes is provided by TOF measurements on the corresponding C_2D_2 adlayer. Within the uncertainty of the present experiments the energy of the E_1 mode was unchanged by this isotopic substitution. For a frustrated translation, this mass change would result in a shift of about 0.2 meV to lower energies, which is too small to be detected. On the other hand, the corresponding energy shift for a frustrated rotation would be 2.3 meV, based on the difference between the rotational constants of the two isotopomers. Since the latter difference, if present, would easily be detected it can be

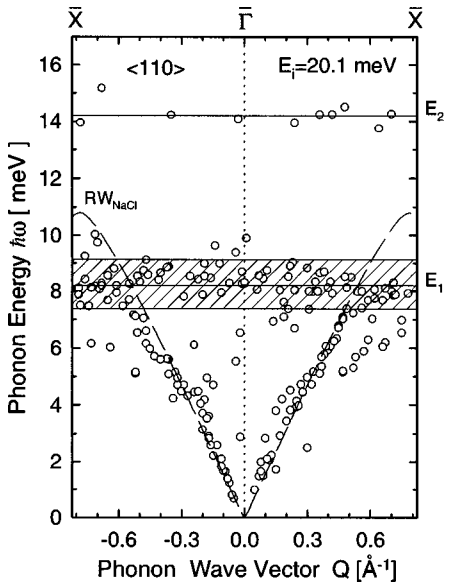

FIG. 4. Surface-phonon-dispersion curves for phase I of acetylene in the ⟨100⟩ direction presented in the reduced zone diagram. The open circles are the measured points. Two horizontal solid lines indicate the Einstein modes attributed to the frustrated translations of C_2H_2 molecules. The dashed sine curve is a model of the substrate Rayleigh mode. The striped zone represents the width of the Einstein mode E_1.

ruled out. As a result, the E_1 mode can be assigned to the frustrated translation of the acetylene adlayer. Unfortunately, the E_2 mode was not detected for the C_2D_2 adlayer and thus an exact assignment of this mode is not possible.

III. THEORETICAL CALCULATIONS

A. Potential energy

The total interaction energy between the C_2H_2 molecules and the NaCl substrate can be written as a sum of the molecule-substrate (V_{MS}) and of the lateral molecule-molecule (V_{MM}) interactions. In the present study, V_{MS} is approximated by the sum of the electrostatic, induction, and dispersion-repulsion interactions between a rigid substrate and rigid acetylene, namely,

$$V_{MS}=V_{MS}^{E}+V_{MS}^{I}+V_{MS}^{DR}. \tag{2}$$

The electrostatic contribution to V_{MS} is modeled by including many electrostatic interactions between the charges of the substrate ions ($q_s=\pm 1$) and a set of point electric multipoles (charges, dipoles, quadrupoles, octupoles, and hexadecapoles) distributed on the C and H atoms of the acetylene molecule (Table I).[15] This distributed description of the electrostatic molecular multipoles (DMA) has been extensively discussed elsewhere[33,34] and accounts for the nonlocal character of the electronic distribution in the molecule. It is well adapted to extended molecules like C_2H_2 and converges rapidly, being more accurate than the usual molecular multipolar distribution for the same number of parameters.

The induction contribution (V_{MS}^{I}) is weak for this system. The dispersion-repulsion interaction (V_{MS}^{DR}) is described by a sum of pairwise Lennard-Jones potentials between the C, H, Na, and Cl atoms. The ϵ and σ parameters for the hetero-nuclear pairs were estimated from the usual pairwise combination rules on homoatomic species and their values are given in Table II. The corresponding parameters for C and H come from the study of Ferry *et al.* on the C_2H_2/MgO system,[15] whereas the ϵ and σ parameters for Na^+ and Cl^- were taken from the study of Wassermann *et al.* on the adsorption of water on NaCl.[5] The substrate parameters were adjusted by 10% to get better agreement with the *ab initio* adsorbate energies of Allouche[8] and the experimental value of the isosteric heat of adsorption.[19] This adjustment had no effect on the equilibrium positions and orientations of the molecules.

TABLE I. Distributed multipole analysis of the acetylene molecule, in atomic units (from Ref. 15).

	H	C	C	H
Charge	0.108	−0.108	−0.108	0.108
Dipole	0	−1.012	1.012	0
Quadrupole	0	−0.501	−0.501	0
Octupole	0	−3.345	3.345	0
Hexadecapole	0	1.329	1.329	0

The interaction between the admolecules (V_{MM}) is written in a similar manner, namely

$$V_{MM}=V_{MM}^{E}+V_{MM}^{I}+V_{MM}^{DR}, \tag{3}$$

where V_{MM}^{E} represents the interaction between the distributed multipoles of two acetylene molecules, V_{MM}^{I} characterizes the mutual polarization, and V_{MM}^{DR} describes the dispersion-repulsion interaction between the atoms of each molecule, written as a sum of pairwise atom-atom Lennard-Jones interactions.

To summarize, the total interaction between the C_2H_2 molecules and the NaCl substrate is written as

$$V=\sum_i \left[V_{MS}(\mathbf{r}_i,\mathbf{\Omega}_i)+\sum_{j\neq i} V_{MM}(\mathbf{r}_i,\mathbf{\Omega}_i,\mathbf{r}_j,\mathbf{\Omega}_j)\right], \tag{4}$$

where $\mathbf{r}_i$ defines the position of the center of mass and $\mathbf{\Omega}_i$ the orientation of the ith molecule in an absolute frame tied to a cation of the surface (Fig. 5).

B. Equilibrium structures

The equilibrium structures of the adsorbate were determined by minimizing the potential energy V with respect to the positions $\mathbf{r}_i=(x_i,y_i,z_i)$ and orientations $\mathbf{\Omega}_i=(\theta_i,\phi_i)$ of

TABLE II. Lennard-Jones potential parameters.

	ϵ (meV)	σ (Å)
C-C	3.69	3.21
H-H	2.13	2.53
C-H	2.81	2.87
Na-C	1.85	3.50
Na-H	1.41	3.12
Cl-C	2.22	3.94
Cl-H	1.69	3.56

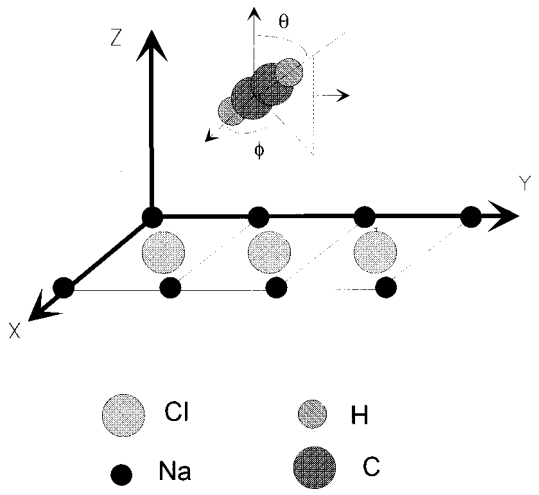

FIG. 5. Geometry of the (001) surface of NaCl. The C_2H_2 molecular orientation (θ,ϕ) is referred to the absolute frame $(\mathbf{X},\mathbf{Y},\mathbf{Z})$.

the admolecules, by using a conjugate gradient method.[35] Whereas for single C_2H_2 molecules adsorbed on NaCl the procedure is straightforward, for monolayer structures the search strategy for finding the minimum-energy configurations is more complex. As a starting point geometries that display a low-order commensurability are used. The (1×1) unit cell can be disregarded as it leads to unstable molecular configurations either due to the repulsive nature of the lateral interactions for a flat geometry or due to the weak interactions associated with molecular geometries corresponding to the acetylene being upright. As a result, the smallest unit cell that is consistent with attractive lateral interactions is the $(\sqrt{2}\times\sqrt{2})R45°$ cell containing two molecules with different orientations. To consider larger cells such as $(m\sqrt{2}\times n\sqrt{2})R45°$, where m and n are integers as in the experimentally determined $(7\sqrt{2}\times\sqrt{2})R45°$ structure, m was increased from 2 to 7 with n equal to 1. The number 7 corresponds to the minimum periodicity for a C_2H_2 plane structure isolated from the bulk that is in registry with the (100) NaCl surface, since the misfit between adjacent molecules is about 8%.[36] The density of these calculated phases corresponds to the full monolayer with all the Na sites being occupied. In a second step, the number N_s of molecules per unit cell was varied to determine the stability of submonolayer phases having the same unit cell $(m\sqrt{2}\times n\sqrt{2})R45°$, but containing a restricted number of molecules. Especially, the high-temperature $(3\sqrt{2}\times\sqrt{2})R45°$ structure containing $N_s=4$ or 2 molecules per unit cell was considered.

The minimization procedure then consisted of a numerical search for the potential minimum associated with these phases with respect to the $5N_s$ degrees of freedom in the unit cell. To avoid trapping into local minima, the minimization was carried out for a large number of initial configurations (about 10^3), making the numerical search of the minimum-energy structure very time consuming, but more likely to give the global minimum for the adlayer.

C. Monolayer dynamics

A theoretical analysis of the phonon-libron dynamics for the monolayer can be used to assign the dispersion curves resulting from the time-of-flight experiments to particular motions of the adsorbate and to explain the coupling between the molecular motions. The calculation method has been presented elsewhere[10,37] and is only briefly summarized here. Only the uncoupled approximation was used, since it has been shown[37] that the coupling between the adlayer motions and the substrate phonons does not dramatically affect the general shape of the dispersion curves.

The Hamiltonian for the external adlayer motions on the rigid substrate is written as

$$H_E=\sum_{\alpha,r,m}\frac{p_\alpha^2(r,m)}{2A_\alpha}+\sum_{\alpha,r,m}\sum_{\alpha',r',m'}\left[\phi^{\mathrm{MM}}_{\alpha,\alpha'}(r,m,r',m')+\sum_{l,s,p}\phi^{\mathrm{MS}}_{\alpha,\alpha'}(r,m,l,s,p)\,\delta_{r,r'}\delta_{m,m'}\right]\times u_\alpha(r,m)u_{\alpha'}(r',m'), \tag{5}$$

where $u_\alpha(r,m)$ and $p_\alpha(r,m)$ are the displacement and the momentum, respectively, associated with the αth variable of the mth molecule in the rth unit cell of the monolayer. When the molecular translations are considered $(\alpha=x,y,z)$, A_α is used both for the molecular mass $(A_x=A_y=A_z=4.32\times10^{-23}$ g molecule$^{-1})$ or for the moment of inertia I or $I\sin^2\theta$ $(I=23.78\times10^{-40}$ g cm^2 molecule$^{-1})$ in which case α characterizes the orientational motions $(\alpha=\theta$ or $\phi)$. ϕ^{MM} defines the lateral force constant tensor that correlates the motions of two molecules and ϕ^{MS} represents the holding force constant tensor due to the static substrate.

The dispersion curves for the monolayer phonons and librons are then obtained by diagonalizing the $(5N_s\times5N_s)$ dynamical matrix $\underline{D}$ connected to the Hamiltonian H_E. This matrix $\underline{D}$ is defined as

$$D_{\alpha\alpha'}(m,m',\mathbf{Q})=\sum_{r'}(A_\alpha A_{\alpha'})^{-1/2}\left[\phi^{\mathrm{MM}}_{\alpha,\alpha'}(r,m,r',m')+\sum_{l,s,p}\phi^{\mathrm{MS}}_{\alpha,\alpha'}(r,m,l,s,p)\,\delta_{r,r'}\delta_{m,m'}\right]\times e^{-i\mathbf{Q}\cdot[\mathbf{R}(r)-\mathbf{R}(r')]}, \tag{6}$$

where $\mathbf{Q}$ is the two-dimensional wave vector in the plane (x,y) of the layer and $\mathbf{R}$ represents the position of the rth unit cell with respect to the origin unit cell. The diagonalization of $\underline{D}$ gives a set of $5N_s$ eigenvalues $\omega_\lambda(\mathbf{Q})$ which correspond to the frequencies of the phonon-libron motions. From the eigenvectors $\mathbf{e}(m,\mathbf{Q},\lambda)$ associated with the frequencies $\omega_\lambda(\mathbf{Q})$ the total spectral density ρ (Ref. 38) is calculated:

$$\rho_{\alpha,\alpha}(\omega)=\sum_{\lambda,m,\mathbf{Q}}|e_\alpha(m,\mathbf{Q},\lambda)|^2\delta(\omega-\omega_\lambda(\mathbf{Q})). \tag{7}$$

IV. THEORETICAL RESULTS

A. Single C_2H_2 molecule

Figure 6 shows the potential energy surface and the equipotential map for a single C_2H_2 molecule as it moves across the NaCl surface. The most stable adsorption site is found

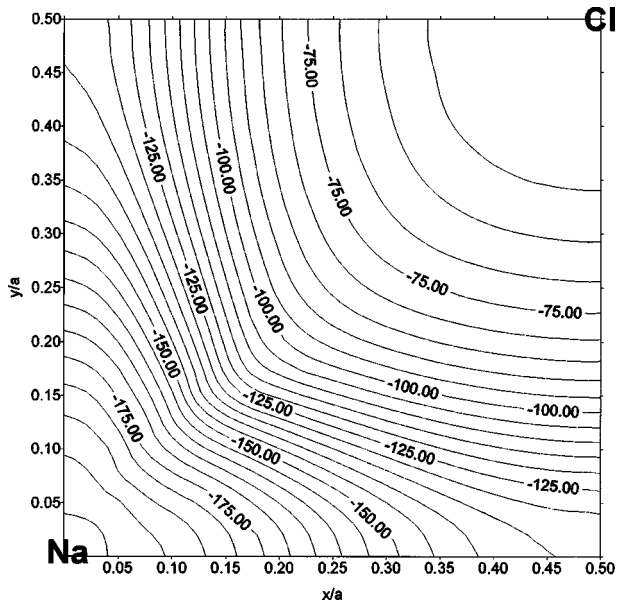

FIG. 6. Equipotential map experienced by the C_2H_2 admolecule above NaCl. The origin ($x=0,y=0$) corresponds to a Na site, whereas $x/a=0.5$ ($a=3.96$ Å) defines the site between two consecutive Na atoms. The molecule lies flat above a Na site with its center of mass located at a distance $z=3.04$ Å from the surface. Energy is in meV and distances are in reduced units of $a=3.96$ Å.

above the Na^+ cation with the molecule lying flat at a distance $z=3.04$ Å from the surface plane with the protons pointing toward nearest-neighbor Cl^- anions. In this configuration, the potential energy is equal to -198 meV. At this same site a secondary energy minimum exists in which the molecules lie parallel to the Na rows. The energy is only slightly higher (-195 meV) and the molecule-surface distance is slightly smaller (2.99 Å). Above the Cl^- site, the molecule lies perpendicular to the surface, with a much weaker interaction of -52 meV. The lowest-energy path along the surface is along the Na rows with an energy barrier of 64 meV. Thus, at $T_S \leqslant 100$ K the molecule remains essentially trapped above the stable Na site with little diffusion across the surface.

B. Acetylene monolayer

For the $(m\sqrt{2}\times n\sqrt{2})R45°$ monolayers, the energy minimization was first performed for low (m,n) values. For $m=n=1$, the calculations lead to a very stable structure containing two inequivalent molecules per unit cell. These molecules are adsorbed on two adjacent Na sites at the same height above the surface ($z=3.03$ Å), with their molecular axes being parallel to the surface and having a relative orientation $\Delta\phi=|\phi_1-\phi_2|$ of about 33°. The molecules are related by a glide plane along the ⟨100⟩ direction. The mean energy V per molecule is equal to -337 meV. Upon increasing m and n to 3 one obtains larger cells with the same adsorbate density that still contain only two inequivalently adsorbed molecules. Every cell in these phases corresponds to a juxtaposition of $(\sqrt{2}\times\sqrt{2})R45°$ geometries. Since the helium diffraction pattern indicates a $(7\sqrt{2}\times\sqrt{2})R45°$ phase,[22] this structure that contains 14 molecules per unit cell

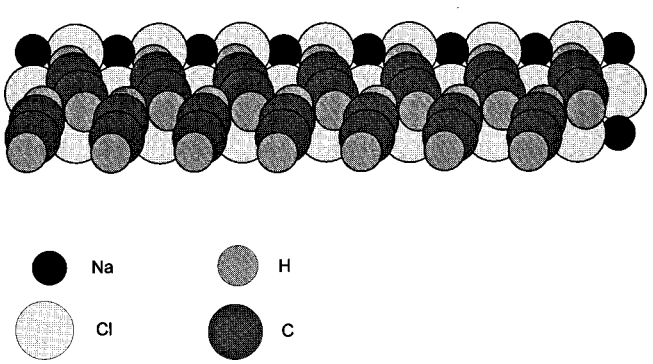

FIG. 7. Minimum-energy configuration for the acetylene molecules in the high coverage phase on NaCl(001) (phase II). This configuration contains a glide plane along the ⟨100⟩ direction.

was carefully investigated. Because this involved altogether 70 degrees of freedom the minimization process was very time consuming. The most stable structure is similar to the $(\sqrt{2}\times\sqrt{2})R45°$ phase (Fig. 7), and does not agree with the observed high-order commensurate structure. To interpret this discrepancy, the $(7\sqrt{2}\times\sqrt{2})R45°$ phase was reexamined by fixing the positions (x,y) of the admolecules above the cations and minimizing the z, θ, and ϕ variables. Moreover, the experimentally observed glide plane was imposed as a constraint, in order to reduce the number of minimization variables. The histogram in Fig. 8 exhibits the distribution over mean total energy for 655 runs starting from different random initial orientations and z positions. The absolute minimum with a mean energy per molecule equal to -337 meV corresponds to the $(\sqrt{2}\times\sqrt{2})R45°$ structure. The histogram clearly shows that other minima with nearly similar energies exist for this full monolayer. For instance, the structure corresponding to the most intense peak, with an energy of -336.5 meV per molecule, contains 12 molecules oriented strictly parallel to the surface at a distance of 3.03 Å from the surface, whereas the two other molecules are slightly higher ($z=3.05$ Å) and tilted by 5° away from the

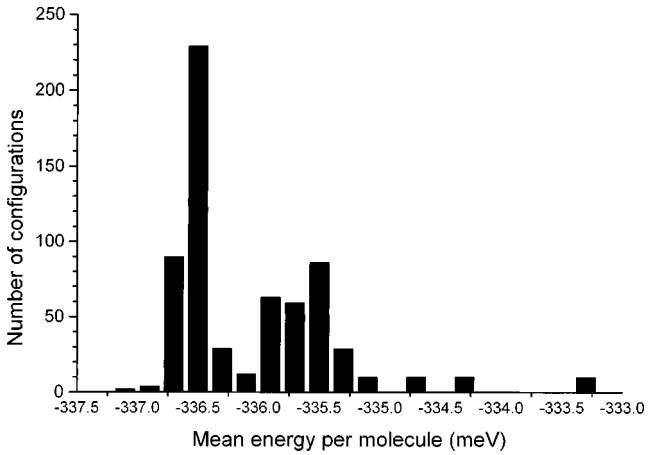

FIG. 8. Histogram of the minimum-energy distribution issued from the minimization procedure for the phase II of acetylene on NaCl(001). The absolute minimum energy is located at -337 meV per molecule whereas the peak at -336.5 meV corresponds to the most probable configuration.

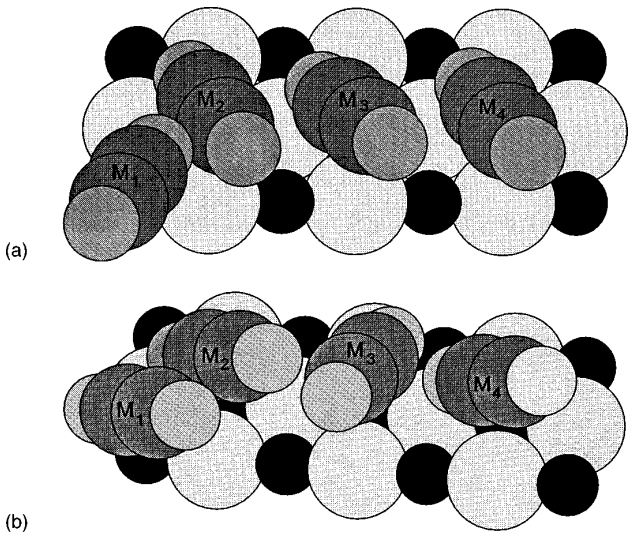

FIG. 9. (a) Minimum-energy configuration (structure *a*) for the molecules in the low coverage phase of acetylene on NaCl(001) (phase I). (b) Secondary minimum-energy configuration (structure *b*) for the same monolayer.

surface plane. Note that the angle $\Delta\phi$ between two adjacent molecules always remains equal to 33°. This configuration results from the competition between the molecule-substrate potential, which favors a strictly flat geometry for the admolecule at an optimized distance of approximately 3 Å, and the lateral interaction, which is optimized when adjacent molecules are perpendicular to each other. In such a case, the molecules cannot lie in the same plane, in order to reduce the repulsion due to the steric effect. Such a structure, like others in the same energy range, exhibit such a buckling with two inequivalent positions and orientations of some molecules. The small energy difference between the low-order commensurate $(\sqrt{2}\times\sqrt{2})R45°$ structure and the buckled high-order phase $(7\sqrt{2}\times\sqrt{2})R45°$ of only 0.5 meV is clearly not significant at finite temperature ($kT=7$ meV at 80 K) and can easily be compensated for by entropy effects. Therefore, although the $(\sqrt{2}\times\sqrt{2})R45°$ configuration has the lowest energy at 0 K, it is very likely that at 80 K the structure with the lowest enthalpy would not be stable. This could explain the experimental results.

Next, the $(3\sqrt{2}\times\sqrt{2})R45°$ low coverage phase, which contains 2 or 4 molecules per unit cell, was studied. Due to the decrease of the lateral interactions, the $N_s=2$ structure is considerably less stable than for $N_s=4$. For this phase, the minimum-energy structure (structure *a*) is given in Fig. 9(a). The centers of mass of the C_2H_2 molecules are still located above Na atoms, and the four molecules lie nearly flat on the surface, at a molecule-surface distance equal to about 3.0 Å. The molecular axes are oriented along the Na rows and the angle $\Delta\phi_{12}$ between the molecules M_1 and M_2, located on adjacent Na sites, is 72° [see Fig. 9(a) for the notation]. Molecules M_2, M_3 and M_4 are adsorbed on second-nearest-neighbor Na sites, M_2 and M_4 being equivalent, while the angles $\Delta\phi_{23}$ and $\Delta\phi_{34}$ are equal to 15°. The mean energy per molecule for this submonolayer structure is approximately -293 meV, indicating a reduction in the stability of 44 meV when compared to the full layer. A secondary minimum (structure *b*) is also found in the calculations [Fig. 9(b)], with an energy per molecule equal to -285 meV. For this minimum, the molecules are still adsorbed above Na atoms, at about 3.04 Å from the surface. Molecules M_1, M_2 and M_4 are equivalent, being nearly parallel to Na-Cl rows, while molecule M_3 makes an angle of 58° with respect to the others.

C. Monolayer dynamics

Figure 10 shows the dispersion curves for the external vibration modes of the $(3\sqrt{2}\times\sqrt{2})R45°$ C_2H_2 layer (structure a) adsorbed on the rigid NaCl substrate along the $\langle 110\rangle$ direction. These curves are calculated by diagonalizing the dynamical matrix $\underline{D}$ [Eq. (6)]. Since the unit cell contains four molecules, $\underline{D}$ is a (20×20) square matrix that gives 20 dispersion curves. The Q values range from 0 to $\pi/3a\sqrt{2}$, where a is the substrate unit-cell parameter, but to allow a direct comparison with the experimental data, the Brillouin zone is extended up to the value $\pi/a\sqrt{2}$, which corresponds to the substrate zone boundary in this direction. The dispersion curves are located in the energy range 3–23 meV and they are characterized by a dispersionless behavior. Two distinct frequency regions are seen between 4 and 10 meV and between 13 and 19 meV. The absence of acoustic modes is the consequence of the substrate corrugation which rules out the translational invariance valid for a floating monolayer. Superimposed on these dispersion curves, the three acoustic branches of the NaCl substrate are depicted by the dotted curves indicating in order of increasing slope the Rayleigh mode, the projection of the transverse acoustic bulk mode and longitudinally polarized surface mode.[37]

The 20 branches were analyzed for the polarizations of the eigenvectors of the dynamical matrix for each Q value. Hence, we give on the right side of Fig. 10 the perpendicular and parallel to the surface spectral densities [Eq. (7)]. Even though the dynamical coupling between neighboring molecules leads to hybridization of the different molecular motions, some general features can be drawn from this analysis. For instance, at $\mathbf{Q}=0$, the third molecule in the unit cell is less coupled to the others [Fig. 9(a)], meaning that its external motions can be considered as pure modes to a first approximation, i.e., modes that are not mixed with the motions of the other three molecules in the unit cell. The dispersion curves associated with the (θ) angular motion are located at around 16 meV, while those around 9 meV are due to the ϕ motion and those around 7 meV to the perpendicular z motion. The x and y parallel motions (see Fig. 5) correspond to curves located, respectively, near 4 and 4.5 meV. For the three other molecules in the unit cell, the highest frequencies (curves at 19 and 23 meV) correspond to ϕ motions and are the consequence of the strong orientational trapping of the molecules due to the lateral interactions with their neighbors. The curves ranging from 13 to 15 meV correspond to the θ motions, whereas the intermediate frequencies between 7 and 9 meV, can be attributed to the z motions. Finally, the curves between 3 and 6 meV are due to the parallel x and y motions of the molecules. At least four peaks occur in the perpendicular contribution within the range 13–16 meV and a single broad peak is present around 7.5 meV, which correspond to z and θ motions, respectively. In contrast, the par-

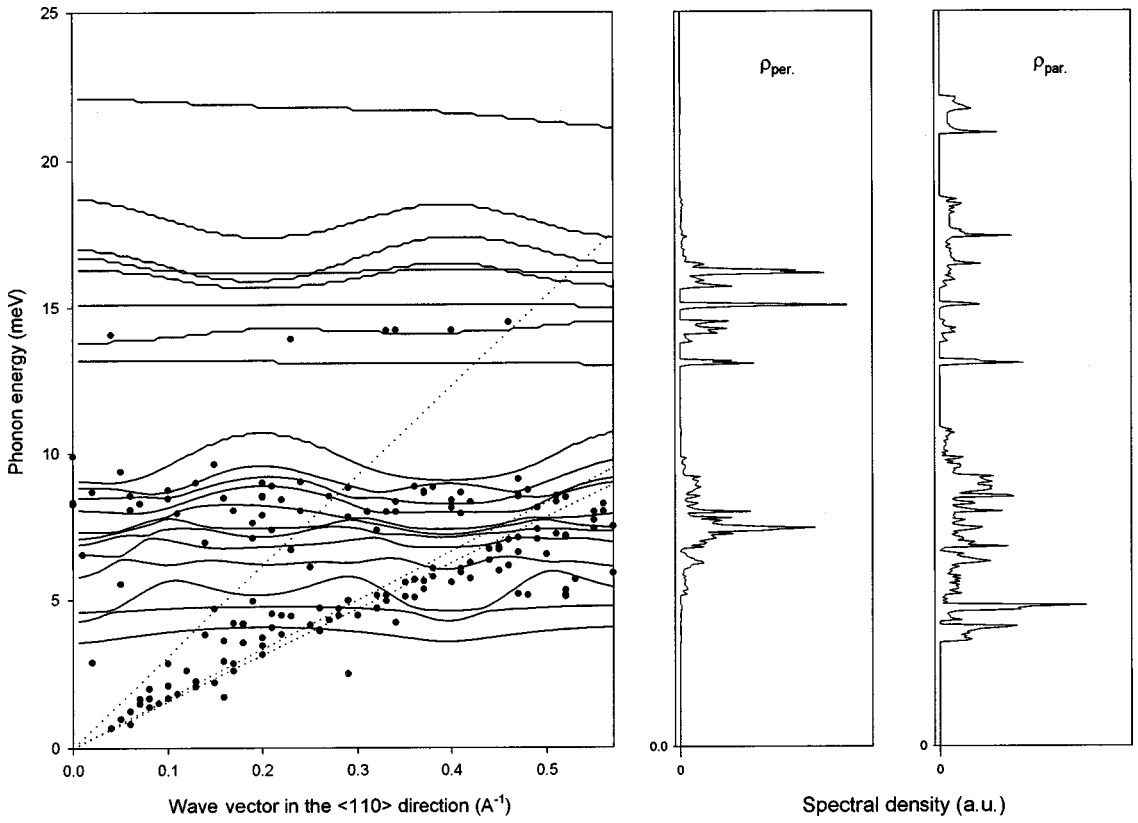

FIG. 10. Dispersion curves for the C_2H_2 submonolayer adsorbed on NaCl(001) (phase I). Full curves represent calculations while points correspond to the experimental data (cf. Fig. 4). In the calculated spectral density of phonon states given in the right side of the figure, we separate the contribution of the modes perpendicular to the surface from the modes parallel to the surface.

allel contribution of the spectral density tends to be more spread out, with structures in the range 3–9 meV characteristic of x and y motions and in the range 13–30 meV characterizing ϕ motions.

The corresponding dynamical study of structure b [Fig. 9(b)] does not provide additional features. The dispersion curves of this structure (not presented here) are not significantly different from those of structure a. This is in agreement with the fact that the molecule-substrate interactions are dominant at these low coverage phases. Since the perpendicular motions are primarily determined by the molecule-surface interactions, the perpendicularly polarized dispersion curves do not change for structures a and b. In contrast, the lateral interactions influence the parallel motions of the admolecules, leading to a slightly different shape for the parallel dispersion curves, which so far has not been experimentally observed.

V. DISCUSSION AND COMPARISON WITH EXPERIMENTS

For the single admolecule, the molecule-substrate interactions favors a stable adsorption site above the cation with a flat orientation of the molecule above the surface with its axis pointing toward the Cl^- anion. The calculated adsorption energy of -198 meV at a molecule-surface distance $z=3.04$ Å, compares fairly well with the parameters for the same configuration from periodic Hartree-Fock (PHF) calculations[8] of -199 meV and $z=3.10$ Å, respectively. However, in the PHF calculations a lower energy (-212 meV) (Ref. 8) is obtained when the molecular axis lies along the Cl-Na-Cl bisector, at a distance of $z=2.74$ Å above the surface plane ions. In the present calculations, this configuration appears as a secondary minimum, with an energy of -195 meV and a distance of $z=2.99$ Å. Moreover, the perpendicular orientation of the molecule above the anion site appears to be stable with an energy of -204 meV in the PHF calculation,[8] while the present calculations predict only a weak bonding of -52 meV. The major reason for this discrepancy has to do with the relative weight of the electrostatic and dispersion-repulsion interactions, since the electron transfer between the molecule and the surface is negligible and the absolute value of the adsorption energy is similar in the two calculations. On the one hand, the accuracy of the semiempirical approach depends crucially on the knowledge of the potential parameters; for the C_2H_2/NaCl system, these parameters seem to be relatively well known. On the other hand, the polarization contribution in the *ab initio* method is only included through second-order perturbation (Moeller-Plesset) and could be significantly underestimated.[8] The dispersion contribution tends to favor a parallel configuration for the admolecules. It is interesting to note that at least for higher coverages the perpendicular orientation for the molecule disagrees with the p over s ratio of the polarized IR signals, which indicates a nearly parallel orientation of the molecular axes.[19]

For the monolayer, the relative stability of a number of $(m\sqrt{2}\times n\sqrt{2})R45°$ phases was investigated using a semiempirical potential model. The possibility of investigating many possible configurations is a major advantage of semiempirical potentials. The low coverage $(3\sqrt{2}\times\sqrt{2})R45°$ phase (phase I) contains four molecules per unit cell (each third substrate ion pair is not occupied), whereas there is one molecule per site in the $(7\sqrt{2}\times\sqrt{2})R45°$ unit cell of the high coverage phase (phase II). The adsorption energy equal to -293 meV per molecule in phase I compares quite well with the experimental heat of adsorption equal to -311 meV per molecule measured by Dunn and Ewing at 78 K at half coverage.[19] For phase II, where all the sites are occupied, the energy per molecule (-337 meV) is in close agreement with the adsorption energy calculated by Allouche for a full coverage (-346 meV per molecule).[8] Moreover, the calculated averaged lateral molecule-molecule interaction energy of -141 meV compares very well with the *ab initio* value (-135 meV).[8] The optimized geometry for this latter phase differs from the one inferred by Allouche,[8] with the mutual angle $\Delta\phi$ between the molecular axes being close to 35° instead of perpendicular, as was inferred in the *ab initio* calculations from symmetry and density arguments. Nevertheless, it should be noted that at 0 K both the structure calculated in the present study and the structure deduced from *ab initio* calculations look like a $(\sqrt{2}\times\sqrt{2})R45°$ geometry instead of the $(7\sqrt{2}\times\sqrt{2})R45°$ phase II structure deduced from the HAS experiments.[22] Phases which exhibit a buckling like the $(7\sqrt{2}\times\sqrt{2})R45°$ structure may, however, be more probable at finite temperatures in close agreement with the observed superstructures in the HAS diffraction pattern. The flat orientation found for the molecules in both phases I and II is consistent with the intensity ratios of the polarized infrared bands.[19] Nevertheless, a careful theoretical study of the infrared response of these two phases would be needed to interpret the experimental signals in more detail. Such an analysis would require the knowledge of the internal vibrational dependence of the potentials for this system. Nevertheless, we can explain qualitatively the presence of three infrared peaks associated with the $(3\sqrt{2}\times\sqrt{2})R45°$ structure. The singlet can be assigned to the M_3 molecule signal [Fig. 9(a)] while the doublet would correspond to M_1 and M_2 or M_1 and M_4 coupled vibrations that are twofold degenerate since the two molecular pairs experience the same surrounding. However, the lack of accurate information on the vibrational dependence of the potential parameters prevents a detailed calculation of the infrared spectrum and, moreover, there may be differences in the experimental conditions for the HAS and PIRS measurements.

To complement the understanding of the C_2H_2 adsorption on NaCl, the external vibrations of the molecules in phase I have been studied both theoretically, on the basis of the dynamical matrix formalism, and experimentally by using inelastic helium-atom spectroscopy. In the experiments, two frequency ranges are observed, between 7 and 9 meV (E_1), and around 14 meV (E_2). The E_1 mode appears at nearly the same energy for C_2D_2 overlayers, leading to the experimental assignment to the frustrated z translation of the acetylene layer. The comparison between the calculated phonon modes and the corresponding experimental data is given in Fig. 10. The higher-frequency modes are not observed since the incident energy of the helium atoms (20.1 meV) is not sufficient to excite high-frequency modes with a large probability. Moreover, the study of the polarization of these modes shows that they correspond primarily to ϕ motions, i.e., to parallel motions since the molecules are flat on the surface. It is well known that HAS experiments are more sensitive to perpendicular than to parallel motions.[39,40] Conversely, the modes between 13 and 14 meV, which are at the limit of the experimental sensitivity, are assigned to θ motions, i.e., perpendicular motions, and can be assigned to the E_2 branch. In the same way, the intermediate frequency modes, ranging between 7 and 9 meV, are connected to z perpendicular motions and are clearly observed in the experimental results as the E_1 branch. Below 5 meV, the experimental points coincide nicely with the substrate acoustic modes (dotted lines in Fig. 10). In the uncoupled dynamical approximation used here, the dispersion curves for the x and y translations of the monolayer, which lie in this energy range between 3 and 6 meV, should be suppressed in the HAS TOF spectra because of their parallel polarization. However, the coupling between the adlayer and the substrate phonons leads to avoided crossings between the corresponding curves near resonances, and through hybridization may change the polarization of the phonon modes.[37] This can explain that the low-frequency modes, which are mainly parallel modes at the center of the Brillouin zone become visible near the zone boundary after hybridization with the perpendicularly polarized Rayleigh substrate mode.

Note finally, that the HAS experiments fail in giving resolvable TOF spectra for the dynamics of phase II. This is probably due to a large number of slightly inequivalent adsorption sites which smears out the peaks. The same difficulty affects the calculations since the large number of molecules per unit cell smears out the dispersion curves.

VI. CONCLUSION

Semiempirical potential calculations have been used to determine the equilibrium structures and the phonon dynamics of the low coverage phase I adlayers of C_2H_2 on the NaCl(001) substrate for comparison with high-resolution helium atom scattering experiments. In this phase, four molecules are adsorbed in the unit cell, above Na sites, with a flat orientation of the molecular axes above the surface. For the full monolayer (phase II) all the cation sites are occupied and the molecules are still parallel to the surface. The large number of degrees of freedom for these large unit cells leads to a distribution of possible structures at 0 K which differ mainly in slight distortions in the θ and z distribution. From a strict potential energy point of view, the most stable full coverage adlayer at 0 K corresponds to a $(\sqrt{2}\times\sqrt{2})R45°$ phase. Nevertheless, this phase undergoes slight distortions due to the dynamical effects with increasing temperature and exhibits a buckling consistent with the registry condition between the layer and the surface, in better agreement with the HAS experiments.[22]

The lattice dynamic calculations make it possible to assign the experimental dispersion curves for the E_1 and E_2

branches obtained from inelastic helium atoms scattering spectra to perpendicular z and θ motions of the molecules in the unit cell, respectively. The other calculated dispersion curves, which correspond mainly to parallel motions within the layers, are only observed because of hybridization with the Rayleigh substrate mode near the Brillouin-zone boundary.

ACKNOWLEDGMENTS

R. E. M. is grateful to the Alexander von Humboldt Society for financial support and acknowledges partial support for this work from the National Science Foundation (CHE-93-18936). We also thank F. Träger and H. Weiss for several valuable discussions.

*Author to whom correspondence should be addressed. FAX: (33)381666475. Electronic address: cgirardet@univ-fcomte.fr

†Permanent address: Department of Chemistry, University of North Carolina, Chapel Hill, NC 27599.

[1] P. N. M. Hoang, S. Picaud, C. Girardet, and A. W. Meredith, J. Chem. Phys. **105**, 8453 (1996).

[2] A. W. Meredith and A. J. Stone, J. Chem. Phys. **104**, 3058 (1996).

[3] C. Girardet, S. Picaud, and P. N. M. Hoang, Europhys. Lett. **25**, 131 (1994).

[4] S. Picaud and C. Girardet, Chem. Phys. Lett. **209**, 340 (1993).

[5] B. Wassermann, S. Mirbt, J. Reif, J. C. Zink, and E. Matthias, J. Chem. Phys. **98**, 10049 (1993).

[6] L. W. Bruch, A. Glebov, J. P. Toennies, and H. Weiss, J. Chem. Phys. **103**, 5109 (1995).

[7] K. Jug and G. Geudtner, Surf. Sci. **371**, 95 (1997).

[8] A. Allouche, Surf. Sci. **374**, 117 (1997).

[9] P. N. M. Hoang, S. Picaud, and C. Girardet, Surf. Sci. **360**, 261 (1996).

[10] C. Girardet, P. N. M. Hoang, and S. Picaud, Phys. Rev. B **53**, 16 615 (1996).

[11] C. Minot, M. A. Van Hove, and J. P. Bibérian, Surf. Sci. **346**, 283 (1996).

[12] G. Pacchioni, Surf. Sci. **281**, 207 (1993).

[13] Y. Ferro, A. Allouche, F. Cora, C. Pisani, and C. Girardet, Surf. Sci. **325**, 139 (1995).

[14] M. I. McCarthy, G. K. Schenter, C. A. Scamehorn, and J. B. Nicholas, J. Phys. Chem. **100**, 16989 (1996).

[15] D. Ferry, J. Suzanne, P. N. M. Hoang, and C. Girardet, Surf. Sci. **375**, 315 (1997).

[16] J. Heidberg, E. Kampshoff, and M. Suhren, J. Chem. Phys. **95**, 9408 (1991).

[17] D. Schmicker, J. P. Toennies, R. Vollmer, and H. Weiss, J. Chem. Phys. **95**, 9412 (1991).

[18] H. C. Chang, H. H. Richardson, and G. E. Ewing, J. Chem. Phys. **89**, 7561 (1988).

[19] S. K. Dunn and G. E. Ewing, J. Phys. Chem. **96**, 5284 (1992).

[20] J. Heidberg, B. Redlich, and D. Wetter, Ber. Bunsenges. Phys. Chem. **99**, 1333 (1995).

[21] D. Ferry, A. Glebov, V. Senz, J. Suzanne, J. P. Toennies, and H. Weiss, J. Chem. Phys. **105**, 1697 (1996).

[22] A. Glebov, R. E. Miller, and J. P. Toennies, J. Chem. Phys. **106**, 6499 (1997).

[23] S. Picaud, C. Girardet, A. Glebov, J. P. Toennies, J. Dohrmann, and H. Weiss, J. Chem. Phys. **106**, 5271 (1997).

[24] L. W. Bruch, M. W. Cole, and E. Zeremba, *Physical Adsorption Forces and Phenomena* (Clarendon, Oxford, 1997).

[25] G. Lange, R. Vollmer, and H. Weiss, J. Chem. Phys. **98**, 10 096 (1993).

[26] J. P. Toennies and R. Vollmer, Phys. Rev. B **44**, 9833 (1991).

[27] A. Glebov, J. P. Toennies, and H. Weiss, Surf. Sci. **351**, 200 (1996).

[28] J. P. Toennies in *Dynamics of Gas-Surface Interaction*, edited by G. Benedek and U. Valbusa, Springer Series in Chemical Physics (Springer, Berlin, 1982), Vol. 21, p. 208.

[29] A. Glebov, J. R. Manson, J. G. Skofronick, and J. P. Toennies, Phys. Rev. Lett. **78**, 1508 (1997).

[30] A. Glebov, W. Silvestri, J. P. Toennies, G. Benedek, and J. G. Skofronick, Phys. Rev. B **54**, 17 866 (1996); G. Benedek, A. Glebov, W. Silvestri, and J. G. Skofronick, J. Vac. Sci. Technol. A **14**, 1522 (1996).

[31] R. B. Doak and D. B. Nguyen, Phys. Rev. B **40**, 1495 (1989).

[32] G. Lange, Ph.D. thesis, 1996 (unpublished). Available from Max-Planck-Institut für Strömungsforschung, Order No. ISSN 0436-1199.

[33] A. J. Stone, Chem. Phys. Lett. **83**, 233 (1981).

[34] A. J. Stone and M. Alderton, Mol. Phys. **56**, 1047 (1985).

[35] P. N. M. Hoang, C. Girardet, M. Sidoumou, and J. Suzanne, Phys. Rev. B **48**, 12 183 (1993).

[36] R. K. McMullan and A. Kvick, Acta Crystallogr., Sect. B: Struct. Sci. **48**, 726 (1992).

[37] C. Girardet, C. Ramseyer, P. N. M. Hoang, and S. Picaud, Phys. Rev. B **52**, 2144 (1995).

[38] V. Pouthier, C. Ramseyer, and C. Girardet, Surf. Sci. **382**, 349 (1997).

[39] J. R. Manson in *Helium Atom Scattering from Surfaces*, edited by E. Hulpke Springer Series in Surface Science (Springer, Berlin, 1992), Vol. 27, p. 173.

[40] D. Eichenauer and J. P. Toennies, J. Chem. Phys. **85**, 532 (1986).